

Thermal Explosion Violence of HMX-Based and RDX-Based Explosives-Effects of Composition, Confinement, and Solid Phase Using the Scaled Thermal Explosion Experiment

J. L. Maienschein, J. F. Wardell

U.S. Department of Energy

Lawrence
Livermore
National
Laboratory

This article was submitted to
Joint Army Navy NASA Air Force 38th Combustions Subcommittee,
26th Airbreathing Propulsion Subcommittee, 20th Propulsion Systems
Hazards Subcommittee and 2nd Modeling and Simulation
Subcommittee Joint Meeting, Destin, FL., April 8-12, 2002

March 14, 2002

DISCLAIMER

This document was prepared as an account of work sponsored by an agency of the United States Government. Neither the United States Government nor the University of California nor any of their employees, makes any warranty, express or implied, or assumes any legal liability or responsibility for the accuracy, completeness, or usefulness of any information, apparatus, product, or process disclosed, or represents that its use would not infringe privately owned rights. Reference herein to any specific commercial product, process, or service by trade name, trademark, manufacturer, or otherwise, does not necessarily constitute or imply its endorsement, recommendation, or favoring by the United States Government or the University of California. The views and opinions of authors expressed herein do not necessarily state or reflect those of the United States Government or the University of California, and shall not be used for advertising or product endorsement purposes.

This is a preprint of a paper intended for publication in a journal or proceedings. Since changes may be made before publication, this preprint is made available with the understanding that it will not be cited or reproduced without the permission of the author.

This work was performed under the auspices of the United States Department of Energy by the University of California, Lawrence Livermore National Laboratory under contract No. W-7405-Eng-48.

This report has been reproduced directly from the best available copy.

Available electronically at <http://www.doc.gov/bridge>

Available for a processing fee to U.S. Department of Energy
And its contractors in paper from
U.S. Department of Energy
Office of Scientific and Technical Information
P.O. Box 62
Oak Ridge, TN 37831-0062
Telephone: (865) 576-8401
Facsimile: (865) 576-5728
E-mail: reports@adonis.osti.gov

Available for the sale to the public from
U.S. Department of Commerce
National Technical Information Service
5285 Port Royal Road
Springfield, VA 22161
Telephone: (800) 553-6847
Facsimile: (703) 605-6900
E-mail: orders@ntis.fedworld.gov
Online ordering: <http://www.ntis.gov/ordering.htm>

OR

Lawrence Livermore National Laboratory
Technical Information Department's Digital Library
<http://www.llnl.gov/tid/Library.html>

THERMAL EXPLOSION VIOLENCE OF HMX-BASED AND RDX-BASED EXPLOSIVES – EFFECTS OF COMPOSITION, CONFINEMENT, AND SOLID PHASE USING THE SCALED THERMAL EXPLOSION EXPERIMENT

Jon L. Maienschein, Jeffrey F. Wardell
Lawrence Livermore National Laboratory
Livermore, CA 94550

ABSTRACT

The Scaled Thermal Explosion Experiment (STEX) has been developed to quantify the violence of thermal explosion under well defined and carefully controlled initial and boundary conditions. Here we present results with HMX-based explosives (LX-04 and PBX-9501) and with Composition B. Samples are 2 inches (50 mm) in diameter and 8 inches (200 mm) in length, under confinement of 7,500 – 30,000 psi (50-200 MPa), with heating rates of 1-3°C/hr. We quantify reaction violence by measuring the wall velocity in the ensuing thermal explosion, and relate the measured velocity to that expected from a detonation. Results with HMX-based explosives (LX-04 and PBX-9501) have shown the importance of confinement and HMX solid phase, with reaction violence ranging from mild pressure bursts to near detonations. By contrast, Composition B has shown very violent reactions over a wide range of conditions.

INTRODUCTION

Development of an understanding of and predictive capability for the hazards involved in thermal explosions of energetic materials exposed to high temperatures such as fires requires that we understand the fundamental reactions of energetic materials exposed to thermal stimuli, and that we quantify the reaction violence that result from these fundamental reactions. With quantified violence data, we can validate computational tools currently being developed and applied to cookoff problems.^{1, 2} The Scaled Thermal Explosion Experiment (STEX), first reported at the 2000 PSHS meeting in Monterey,³ is designed to quantify the violence of thermal explosions under carefully-controlled conditions, to provide a database which we can use to validate predictive codes and models. The use of the STEX data is complemented by separate measurements of fundamental reaction kinetics, such as those reported previously⁴ and in this meeting.⁵

Previous experimental studies of reaction violence have been limited by the available diagnostics to quantify the violence. Many thermal explosion experiments done to date have been screening tests to determine qualitative violence, typically by observing number and size of fragments. Further, the initial and boundary conditions are often not well-known, since screening experiments are generally low-cost, which makes it difficult to tightly control the external and internal conditions. Other experiments have been run at a very small scale; these can be carefully designed to emphasize a particular aspect of thermal reaction, but are difficult to extrapolate to scales more representative of actual systems.

We developed the Scaled Thermal Explosion Experiment (STEX) to address the lack of quantitative data on thermal reaction violence, and reported initial results with HMX-based explosives.³ Here we present additional data with HMX-based materials as well as results with Composition B. We also report on a method to estimate the percent of detonation energy represented by the thermal explosion, which provides a useful comparison of different explosives. The work reported here represents further progress towards our goal to provide a database of violence of thermal explosions for materials of interest under well-controlled conditions, to support the development of a predictive capability for thermal explosion violence.

Approved for public release, distribution is unlimited.

This work was performed under the auspices of the U. S. Department of Energy by the University of California, Lawrence Livermore National Laboratory under Contract No. W-7405-Eng-48.

EXPERIMENTAL APPARATUS AND CONDITIONS

DESCRIPTION OF SCALED THERMAL EXPLOSION EXPERIMENT

The STEX test was developed with the following goals: uniform heating for well-defined boundary condition; well-defined physical confinement; pre-determined reaction location away from end effects; a range of physical scales; quantitative measurements of reaction violence; and design to allow accurate simulations of the system, avoiding physical features that are difficult to model. To this end, we devised a cylindrical test where the reaction initiates in the axially-central region of the cylinder (radial location depends on heating rate). Confinement is provided by a steel wall and end caps with known mechanical properties that are relatively insensitive to temperature. Confinement levels are 7.5, 15, or 30 ksi (50, 100, 200 MPa) set by selecting the thickness of the cylinder wall. For the 2-inch diameter, 8-inch long vessel (50.8 mm diameter, 203 mm length) used in this work, the respective wall thicknesses were 0.040, 0.080, and 0.120 inch (1.02, 2.03, 4.06 mm). Violence is quantified through non-contact micropower impulse radar as well as through strain gauges attached to the cylinder walls. The vessel configuration is shown in

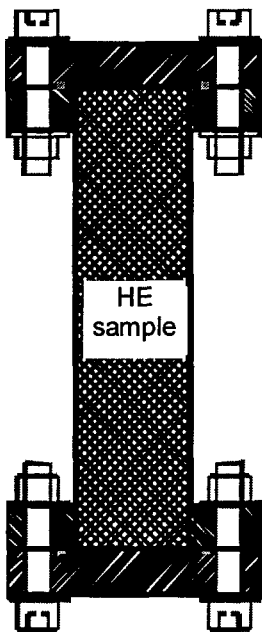


Figure 1. Design of STEX vessel

Figure 1. We reported additional details in the PSHS meeting in Monterey in November 2000.³

Diagnostics include: external temperature at fifteen locations; internal temperature on the center axis of the explosive at five heights; hoop and axial strain of the cylinder wall measured by strain gauges; and wall velocity measured by micropower impulse radar. We use three radar channels to measure wall velocity at three angular locations around the vessel. More detail on these diagnostics was given in our previous paper.³

The vessel is heated with three non-contact radiant heaters under feedback control, chosen to reduce temperature gradients that are typically present with heater bands, and to eliminate the non-quantifiable extra confinement that heater bands provide. Each end cap is heated with a separately-controlled heating element.

For HMX-based explosives, calculations with decomposition kinetic schemes⁶ showed that a heating rate of 1°C/hr is required to locate the ignition point at the center of a 2-inch diameter sample. At the slightly-faster rate of 1.44°C/hr, the calculated ignition point was about 0.4 inch (10 mm) from the edge. Because we expected maximum violence with center-ignited reactions, the experiments with HMX-based explosives run to date have been heated at 1°C/hr from 130°C until thermal explosion occurs, after an initial fast ramp to 130°C and 5-hour equilibration at 130°C. For Composition B, we used final ramp rates of 1, 2, and 3°C/hr.

The mass of explosive must be carefully chosen to allow for thermal expansion and any phase transitions. HMX undergoes a $\beta \rightarrow \delta$ solid-solid phase transition about 160°C,⁷⁻¹¹ while the TNT component of Composition B melts at 80°C with approximately 13% increase in volume.¹² The explosive sample is sized for each experiment so that the sample comes in contact with the confinement either before, during, or after the phase transition, depending on the desired conditions for the experiment.

SAMPLE DESCRIPTION

We have studied two HMX-based explosives with the STEX test. LX-04 contains 85% HMX of trimodal particle size distribution and few large particles (> 100 μm), and 15% Viton A binder. PBX-9501 contains 95% HMX with a trimodal particle size distribution and a significant fraction > 100 μm , with a binder of 2.5% Estane and 2.5% BDNPA/F. Samples for most runs were uniaxially pressed to a density of > 98.5% of theoretical maximum, although samples for runs 1, 3, 6, 7 were pressed isostatically to about the same density. The key differences between these two formulations are the proportion of HMX to binder, and the presence of larger particles in the PBX-9501.

The $\beta \rightarrow \delta$ phase transition in HMX involves a volumetric expansion of about 6% and therefore the phase transition is hindered by high pressure.⁷⁻¹¹ Previously we showed that confining HMX at 30,000 psi (200 MPa) increases the phase transition temperature by over 30°C.³ Therefore, by sizing the explosive sample so that it comes snug with the vessel wall before the phase transition, experiments with 30,000 psi (200 MPa) confinement can be conducted under conditions that prevent the phase transition; in this way, we can study the effect of HMX solid phase on thermal explosion violence. To illustrate the differences required, we compare the sample sizes for PBX-9501 in runs 8 (δ -phase) and 11 (β -phase). For run 8 the PBX-9501 was 1.955 in (49.66 mm) diameter, 7.819 in (198.6 mm) long, with a mass of 706 g; for run 11 the PBX-9501 was 1.9955 in (50.69 mm) diameter, 7.981 in (202.7 mm) long, with a mass of 750 g. For each test, three cylindrical pieces of explosive were stacked to achieve the final height, with the center piece being approximately twice the length of the top and bottom piece; this was designed to ensure that the ignition point at the vertical center of the sample is not at a joint between two pieces. In all cases a hole was drilled along the center axis of the parts to insert the internal thermocouple.

The Composition B used here contained 63% RDX, 36% TNT, and 1% wax. For the first two runs, the material was pressed and machined into cylinders including a hole along the axis for the internal thermocouple, each with diameter of ~1.93 inches (49 mm) and length of ~2.66 inches (68 mm). Each run contained three cylinders, with a total mass of 646 g. For subsequent experiments, the Composition B was cast into the vessel with the internal thermocouple in place, again with a total mass of 646 g. Inasmuch as the TNT melts long before the thermal explosion takes place, there was no need to maintain the accurate and costly dimensional control through pressing and machining as was done for the first two runs.

RESULTS AND DISCUSSION

RELATING REACTION VIOLENCE TO DETONATION

To relate the wall velocity measurements to detonation energy, we turn to the Gurney method. In this approach, for a metal cylinder being expanded by a detonating explosive, the wall velocity can be estimated from the test geometry and a "Gurney energy" that is characteristic of the explosive.¹³

$$V_{wall} = \sqrt{2E} \left(\frac{M}{C} + \frac{1}{2} \right)^{-1/2} \quad (1)$$

where:

$$\frac{M}{C} = \left[\left(\frac{OD}{ID} \right)^2 - 1 \right] \frac{\rho_m}{\rho_c} \quad (2)$$

The quantity $\sqrt{2E}$ is the "Gurney energy", OD and ID are the outer and inner diameter of the metal cylinder, ρ_m is the density of the cylinder wall, and ρ_c is the density of the explosive filling the cylinder. The Gurney energy is tabulated for many explosives undergoing detonation.¹³

Using the wall velocity from the thermal explosion and the test geometry, we can rearrange Eqs.(1) and (2) to calculate a thermal "Gurney energy" $\sqrt{2E_{thermal}}$ for each experiment. We then estimate the percent of detonation energy represented by the thermal explosion by:

$$\text{percent of detonation energy} = \left(\frac{\sqrt{2E_{thermal}}}{\sqrt{2E}} \right)^2 \times 100 \quad (3)$$

This quantity is shown in Tables 1 and 2 for HMX-based explosives and for Composition B, respectively. The quantity "average" wall velocity is calculated using the formula:

$$\text{"average" wall velocity} = \frac{\text{mean velocity}}{\left(1 + \frac{\text{std dev velocity}}{\text{mean velocity}}\right)} \quad (4)$$

which reduces the effect of one very high velocity reading on the overall average. If one radar channel records very high velocity while the others do not, the reaction is most likely not very violent, and Eq.(4) was developed on this basis.

RESULTS WITH HMX-BASED EXPLOSIVES

The results for LX-04 and PBX-9501 are shown in Table 1. Some of these data were included in our earlier paper,³ but our reanalysis of the earlier experiments has resulted in minor changes in some of the numbers. In addition, we made several new runs to replicate conditions of interest (runs 27-29).

Table 1. Summary of scaled thermal explosion experiments with HMX-based explosives. All are 2-inch diameter, 8-inch length (50.8 mm diameter, 203 mm length), with a ramp rate of 1°C/hr above 130°C. Onset temperature is the highest reading on the vessel exterior at the time of runaway reaction. Some vessels were vented prior to thermal explosion, as shown by strain gauge and temperature data and by visual and aural observation. Violence is indicated by fragment distribution, by peak wall velocities measured by radar, by calculation of percent of detonation energy, and by final strain rate.

Test #	Explosive	Confinement, ksi (MPa)	HMX phase	Onset temp., °C	Vented ?	Fragments [†]	Wall velocity (3 channels), m/s	"Average" wall velocity, m/s	% of detonation energy	Log (radial strain rate, s ⁻¹)
1	LX-04	3.8* (25)	δ	173	No	None	13, 0, 0	2	0	-
3	LX-04	7.5 (50)	δ	172	No	None	0, 0, 40	5	0	-
6	LX-04	30 (200)	δ	192	Yes	4L, 4S	800, 200, 400	280	2	3.5
28	LX-04	30 (200)	δ	191	Yes	None	-90, 850, 130	110	0	1.7
9	LX-04	30 (200)	δ	192	No	None	0, 800, 0	98	0	-
29	LX-04	30 (200)	δ	191	No	None	0, 1100, 450	250	2	1.7
7	LX-04	30 (200)	β	187	Yes	1 S	70, 0, 1000	140	0	2.1
10	LX-04	30 (200)	β	188	No	None**	200, 200, 200	200	1	4.1
2	PBX-9501	7.5 (50)	δ	170	No	None††	130, 60***, 130	77	0	-
27	PBX-9501	7.5 (50)	δ	170	No	None	700, 700, 700	700	5	-
4	PBX-9501	30 (200)	δ	169	Yes	5 L, 9 S	600, 800, 200	340	3	-
8	PBX-9501	30 (200)	δ	170	No	6 L, 10 S	300, 800, 700	420	4	-
5	PBX-9501	30 (200)	β	169	Yes	"Detonation"	1700, 1600, 1900	1600	57	4.1
11	PBX-9501	30 (200)	β	165	No	"Detonation"	1400, 1700, 1200	1200	33	4.3

* vessel was 7.5 ksi design, but had flaw in metal allowing failure at lower pressure.

† none – vessel split open; L: large fragments several inches in largest dimension; S: small fragments ~ 1 inch; "detonation" – vessel destroyed, hole punched in end cap, nothing recoverable from cylinder wall;

** Bottom heater failed during run. Reaction initiated above center of vessel, which split into three vertical segments aligned with three radiant heaters.

†† vessel completely split and folded back onto itself.

*** radar 2 recorded motion ~ 2ms later than radars 1 & 3, as the vessel walls folded back into view of radar 2.

Details of the thermal explosion progression may be seen in the internal temperature data preceding and during the thermal explosion. Typical results are shown in Figures 2 and 3 for PBX-9501 (run 27, see Table 1). In Figure 2, the internal temperature data at the middle of the sample shows that slow self-heating had begun even before the clearly-visible endothermic phase transition at 160-164°C. Following the phase transition, slow self-heating resumed and is visible in the upper and lower internal thermocouples as well; eventually the self-heating accelerated to a runaway condition.

The thermal excursion during the explosion is recorded by using a fast scan rate, with all five internal temperatures recorded each second. (The time response of the internal thermocouple, with a wall thickness of 0.016 inch (0.41 mm), is sufficiently slow that a one-second recording period is appropriate.) As shown in Figures 2 and 3, the temperature at the middle is the highest prior to the onset of rapid reaction. However, as the runaway accelerates the location of the highest temperature sometimes shifts.

In Run 27, shown in Figure 3, the reaction moved upward in the vessel, with thermocouples above the middle showing higher temperatures. In other runs, we have seen the reaction move downward. The samples are made as uniformly as is possible, but apparently there is still sufficient inhomogeneity to drive the reaction in different directions in different tests. This effect will be very difficult to capture in computer simulations of thermal explosions.

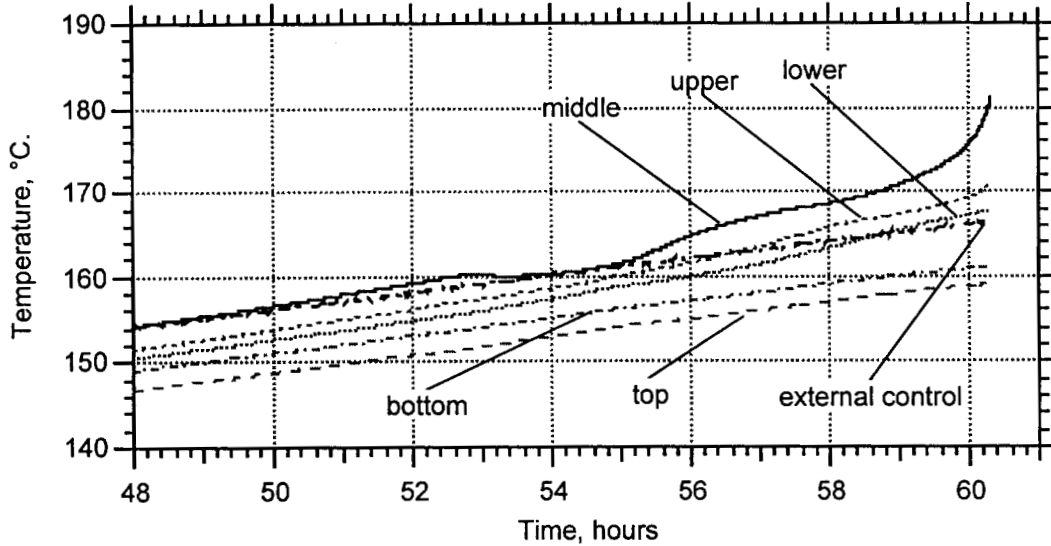


Figure 2. Run 27, PBX-9501: Internal temperatures and external control temperature in final hours preceding thermal explosion. A set of readings was recorded every ~ 50 seconds, so final thermal excursion was not captured.

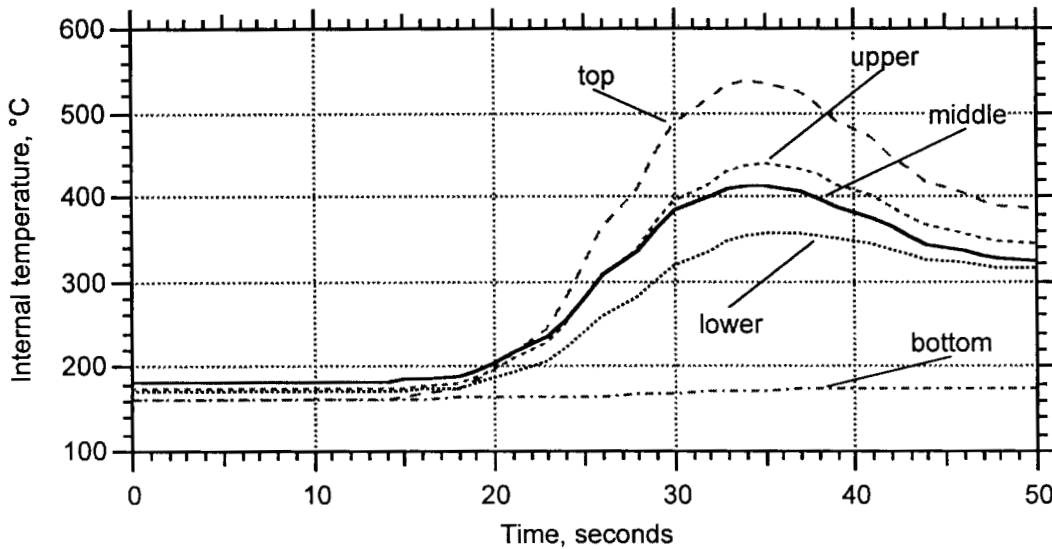


Figure 3. Run 27, PBX-9501: Internal temperatures during thermal runaway and explosion. One set of data was recorded every second. Reaction was sufficiently mild that thermocouples survived the explosion and recorded the cool down afterwards.

The radial and axial strains in the vessel wall are measured with Micrometrics EP-series strain gauges rated for 20% strain; however, the adhesive used (M-bond 610) is rated to about 3% strain and therefore limits the range of our strain measurements. In many experiments we successfully recorded

axial and radial strain during the thermal explosion. The radial strain rate data during the final wall expansion just prior to loss of signal are reported in Table 1 and displayed in Figure 4 compared with the "average wall velocity". In Figure 4 we see that data set for each explosive shows reasonable correlation, but the data sets together show much less correlation. There is uncertainty in both the wall velocity and strain rate results, and we are just beginning to study and understand their correspondence. Also, the strain rate data are preliminary at this point, and further analysis may provide refined values.

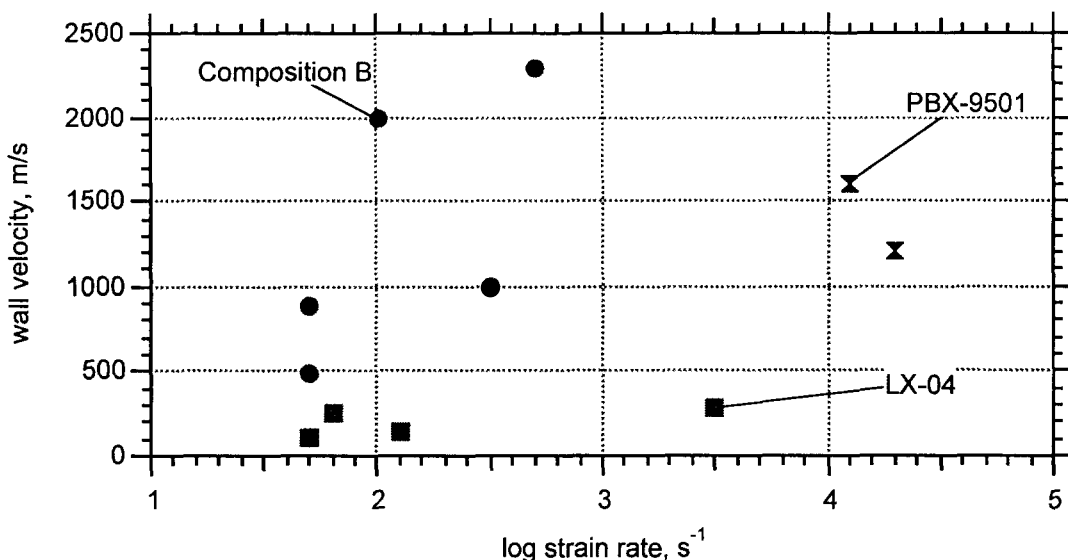


Figure 4. Comparison of "average" wall velocity with radial strain rate in the vessel wall. The strain rate data result from preliminary analysis of the strain data, and may be improved in the future.

We can draw some observations from the entire data set with HMX explosives. The conclusions drawn in the previous paper are still valid. Composition appears to be very significant, since LX-04 (with 15% binder) produces thermal explosions that are consistently less violent than those with PBX-9501 (2.5% binder, 2.5% plasticizer). With LX-04 the maximum percentage of detonation energy is 2% , while with PBX-9501 this is as high as 57%. Effects of confinement are as expected, with higher confinement leading to more violent reactions in both LX-04 and PBX-9501.

The effect of the HMX phase transition is complex. For experiments at low confinement, the phase transition takes place and the reaction involves δ -phase HMX. As discussed above, the phase transition temperature is increased by about 30°C at pressures of 30,000 psi (200 MPa), and therefore the phase transition may be retarded by sizing the sample to come snug with the confinement prior to reaching the phase transition temperature. In this latter case, the confining pressure increases the phase transition temperature sufficiently high that the thermal explosion occurs before the phase transition. The internal thermocouple gives a clear endotherm indicative of the phase transition in the former case with δ -phase, whereas no such feature is seen in the latter case with β -phase. Each experiment in Table 1 is labeled with the final HMX phase prior to thermal explosion.

For LX-04, there is no strong effect of HMX phase, with the violence being about the same for the two phases. We do note that the onset temperature with LX-04 is reduced about 3°C when the phase transition is retarded. For PBX-9501, the effect of HMX phase is profound. In addition to a lowering of the onset temperature of 1-4°C, the nature of the thermal explosion changes completely when the phase transition is retarded. The violence appearing essentially "detonative" with very high wall velocities, holes punched in inch-thick end caps, and complete destruction of the confining cylinder and surrounding diagnostics. For the two replicate runs at this condition, the percentage of detonation energy is quite high, 33-57%. These two runs were the only ones in which a very high degree of violence was seen with HMX-based explosives.

The results in Table 1 are complicated by the fact that some of the experiments were vented, allowing decomposition gases to escape during the heating process. Each run in Table 1 is labeled accordingly. Of the runs labeled as vented, all but run 28 were vented when the internal thermocouple leaked at the top, allowing gas from the top center of the sample to escape through the thermocouple sheath. Run 28, on the other hand, was vented by eliminating the gasket sealing the top flange, allowing gas to escape from the top outer edge of the explosive. This difference in location of the leak proved to be significant, with leakage from the center leading to higher violence with LX-04 (compare run 6 with center leakage and run 28 with edge leakage). Although initially unexpected, this behavior is consistent with modeling results by Larry Luck at Los Alamos National Laboratory, in which he showed that thermal explosion reactions would be expected to be different for cases where gas took different pathways out of the solid.¹⁴

The effects of venting are apparent in the internal thermocouple records, as discussed in our previous paper.³ The recent data are consistent with those shown in the previous paper, and hence will not be repeated here. To summarize the observations: the higher reaction temperature for LX-04 seen in the external temperature data is also seen in the internal data; the endotherm from the $\beta \rightarrow \delta$ phase transition is clearly seen for runs in which the transition was not retarded, and is not seen for runs where it was retarded; and self-heating leads to higher internal temperatures for runs that are vented when compared with similar runs that were not vented. Possible reasons for the increased internal heating with vented runs were presented in our previous paper.³ Regardless of the actual reason, we conclude that gas release through venting leads to higher internal temperatures and, in some cases, more violent thermal explosions. This is counter to intuition saying that venting should lead to less violent reactions.

The quantity reported as the "% of detonation energy" is very low for all experiments with HMX-based explosives, except for the two runs with PBX-9501 under high confinement and with samples sized to maintain the HMX in β -phase. There is clearly a significant difference between the reaction in the latter two runs and those in the other runs with HMX. Our hypothesis is that the phase of the HMX is the difference, and we are continuing efforts to demonstrate (or disprove) this through measurement of the phase present under both types of conditions.

RESULTS WITH COMPOSITION B

Results from several tests with Composition B are shown in Table 2. All runs are with 2-inch (50.8 mm) diameter, with differing confinements and thermal ramp rates. We immediately see that the violence of thermal explosion with Composition B is significantly greater than with HMX-based explosives reported in Figure 1, with almost all reactions giving > 10% of the detonation energy and some giving 100%. Only the run with lowest confinement and fastest ramp rate gave a very low violence as seen from lack of fragmentation (only one fragment ejected) and only one radar channel detecting a (low) wall motion. The wall strain rate was fairly high in this experiment, which would be expected if the strain gauge were located close to where the wall failure began and the fragment formed. The strain rate data for Composition B are included in Figure 4, above, and show a reasonably good correspondence with wall velocity.

OVERALL REACTION VIOLENCE

The overall picture of reaction violence from each experiment must be drawn from consideration of all the diagnostics. It is possible for one diagnostic to record an apparently very violent event, such as if one fragment is ejected directly towards a radar detector or if a strain gauge happens to be located very close to the failure point of the metal wall. Only by having several types of measurements and comparing them can we draw a consistent picture of reaction violence across a set of experiments. The data perhaps most useful to those developing or validating predictive models of thermal explosion are the strain rate in the vessel wall, with wall velocity being somewhat more difficult to interpret and fragmentation data being very difficult because of the not-well-understood nature of metal fracture under these conditions of fairly low strain rates. However, any strain rate data from this or other thermal explosion experiments must be considered against the integrated picture of reaction violence, to ensure that the strain rate data truly represent the behavior of the entire assembly and do not distort the

outcome. If all available data for a particular experiment are consistent, we may use them to quantify the reaction violence. If the data are not consistent, then judgement must be applied in assigning a quantification to reaction violence.

Table 2. Summary of results of scaled thermal explosion experiments with Composition B. For all: 2-inch diameter, 8-inch length (50.8 mm diameter, 203 mm length); ramp rate above 130°C is shown. Onset temperature is the highest reading on the vessel exterior at the time of runaway reaction. All vessels were sealed, with no evidence of venting. Violence is indicated by fragment distribution, by peak wall velocities measured by radar and by calculation of percent of detonation energy.

Test #	Confinement, ksi (MPa)	Ramp rate, °C/hr	Onset temp. °C	Fragments*	Wall velocity† (3 channels), m/s	"Average" wall velocity m/s	% of detonation energy	Log (radial strain rate, s ⁻¹)
12	30 (200)	1.0	159	37	2100, 2000,	2000	100	2.0
13	30 (200)	1.0	160	52	2000, 2800, 1000	1300	45	-
17	30 (200)	2.0	164	48	, 1800, 600	700	13	2.5
18	30 (200)	3.0	166	48	1100, 900,	880	20	1.7
19	15 (100)	1.0	164	22	2500, 2500,	2500	100	2.7
20	15 (100)	3.0	169	1**	200, ,	200	1	1.7

* none: vessel split; L: large frags several in. largest dimension; S: small frags ~ 1 in.; "Detonate": vessel destroyed, hole punched in end cap, cylinder wall unrecoverable.

** vessel wall was largely intact, but greatly deformed. One fragment was ejected.

† in some cases, radar channel did not report. Missing data are shown by inserted commas.

RELATIONSHIP OF THERMAL EXPLOSION VIOLENCE TO DEFLAGRATION BEHAVIOR

In a thermal explosion, ignition at some location begins the deflagration process, with resultant energy release and pressure increase. The increase in pressure then drives the deflagration faster, leading to accelerating rates and eventual explosion. The violence of the explosion depends on the ultimate reaction rates that are attained before the system disassembles in the explosion. Therefore, we expect that the deflagration behavior of an explosive will strongly affect the violence of the ensuing thermal explosion, and we in fact observe this for the materials studied to date.

For HMX-based explosives, we have previously reported that LX-04 exhibits a deflagration rate that is 1st order in pressure up to pressures of 600 MPa, whereas PBX-9501 shows a similar pressure dependence at low pressures but very rapid and erratic deflagration with rates of 10-100x faster at pressures about 100-150 MPa.⁴ Since thermal explosions are driven by deflagration processes, we expect rapid deflagration to lead to violent thermal explosions, and this is what is seen.

With Composition B, we have measured a 2nd order pressure dependence of the deflagration rate, which leads to very rapid acceleration of the deflagration.⁵ In addition, deconsolidation in Composition B samples leads to very high deflagration rates, which will drive the violence even higher.⁵ Therefore, on the basis of the deflagration behavior, we would expect Composition B to give violent thermal explosions, and this is what we observed in these experiments.

SUMMARY AND CONCLUSIONS

The Scaled Thermal Explosion Experiment (STEX), with carefully defined and controlled initial and boundary conditions and extensive diagnostics, is providing detailed information on thermal explosion violence and on the processes leading to the eventual thermal explosion. Clear differences can be seen between formulations containing the same explosive component, such as LX-04 and PBX-9501; these differences must be considered in analysis of hazards engendered by systems containing these or related explosives. The very high violence from Composition B thermal explosions under many conditions shows that the hazards involved with it may be significantly greater.

The STEX experiment was designed with modeling in mind, both in the simplicity and thorough definition of the design and in the provision of extensive diagnostics. The temperature, wall velocity, and

strain rate diagnostics provide data necessary to develop and validate predictive computational models such as is being done by McClelland and coworkers.^{1, 2} As the need is identified for further diagnostics, these may be added to future experiments.

Each experiment generates a large data set including temperatures, strains, and wall velocities, as well as photographs and videos of the experiment set up, execution, and aftermath. These data sets are being compiled, documented, and recorded for distribution to those in the explosive community who may find them useful. If the reader is interested in getting any or all of the data sets, he may contact the first author.

ACKNOWLEDGEMENTS

We would like to thank the following people for their contributions. Al Nichols, Jack Reaugh, Craig Tarver, LeRoy Green, Ed Lee, Matt McClelland, and Tri Tran participated in the conceptual design and development of the STEX test as well as analysis of results. Electronic support has been provided by Dan Greenwood and Greg Sykora. Mechanical and fabrication support has been provided by Les Calloway, and Ed Silva. Tom Rosenbury, Doug Poland, Bob Simpson, and George Governo have provided micropower impulse radar measurements. Bill Gilliam, Larry Crouch, and Denise Grimsley have been very supportive in execution of these experiments in the High Explosives Applications Facility at LLNL.

REFERENCES

1. M.A. McClelland, T.D. Tran, B.J. Cunningham, R.K. Weese and J.L. Maienschein, "Cookoff Response of PBXN-109: Material Characterization and ALE3D Model", in *Proceedings of JANNAF 37th Combustion and 19th Propulsion Systems Hazards Subcommittee Meetings*, Monterey, CA, CPIA Publication 704 Vol I, p. 191 (2000).
2. M.A. McClelland, J.L. Maienschein, A.L. Nichols, J.F. Wardell, A.I. Atwood and P.O. Curran, "ALE3D Model Predictions and Materials Characterization for the Cookoff Response of PBXN-109", in *Proceedings of JANNAF 38th Combustion and 20th Propulsion Systems Hazards Subcommittee Meetings*, Destin, FL, CPIA Publication (2002).
3. J.L. Maienschein, J.F. Wardell and J.E. Reaugh, "Thermal Explosion Violence of HMX-Based Explosives - Effect of Composition, Confinement and Phase Transition Using the Scaled Thermal Explosion Experiment", in *Proceedings of JANNAF 37th Combustion and 19th Propulsion Systems Hazards Subcommittee Meetings*, Monterey, CA, CPIA Publication 704, p. 1-83 (2000).
4. J.L. Maienschein and J.B. Chandler, "Burn Rates of Pristine and Degraded Explosives at Elevated Pressures and Temperatures", in *Proceedings of 11th International Detonation Symposium*, Snowmass, CO, Office of Naval Research, p. 872 (1998).
5. J.L. Maienschein and J.F. Wardell, "Deflagration Behavior of PBXN-109 and Composition B at High Pressures and Temperatures", in *Proceedings of JANNAF 38th Combustion and 20th Propulsion Systems Hazards Subcommittee Meetings*, Sandestin, FL, CPIA Publication (2002).
6. R.R. McGuire and C.M. Tarver, "Chemical Decomposition Models for the Thermal Explosion of Confined HMX, TATB, RDX, and TNT Explosives", in *Proceedings of Seventh Symposium (International) on Detonation*, Annapolis, MD, Naval Surface Weapons Center, p. 56 (1981).
7. H.H. Cady, "Studies on the Polymorphs of HMX", Los Alamos Scientific Laboratory, LAMS-2652 (October 18, 1961).
8. W.C. McCrone, "Crystallographic Data: Cyclotetramethylene Tetranitramine (HMX)", *Analytical Chem.*, **22**, 1225 (1950).
9. A.S. Teetsov and W.C. McCrone, "The Microscopical Study of Polymorph Stability Diagrams", *Microscop. Cryst. Front.*, **15**, 13 (1965).

10. M. Herrmann, W. Engel and N. Eisenreich, "Phase Transitions of HMX and their Significance for the Sensitivity of Explosives", in *Proceedings of the Technical Meeting of Specialists MWDDEA AF-71-F/G-7304 - Physics of Explosives*, p. 12 (1990).
11. R.E. Cobbley and R.W.H. Small, "The Crystal Structure of the δ -form of 1, 3, 5, 6 - Tetranitro-1, 3, 5, 7-tetraazacyclooctane (δ -HMX)", *Acta Cryst.*, **B30**, 1918 (1974).
12. J. Köhler and R. Meyer, *Explosives, Fourth, revised and extended edition*, VCG, Weinham (1993).
13. B.M. Dobratz and P.C. Crawford, "LLNL Explosives Handbook: Properties of Chemical Explosives and Explosive Simulants", Lawrence Livermore National Laboratory, UCRL-52997 change 2 (January 31, 1985).
14. L. Luck, Los Alamos National Laboratory, personal communication, October 2001.